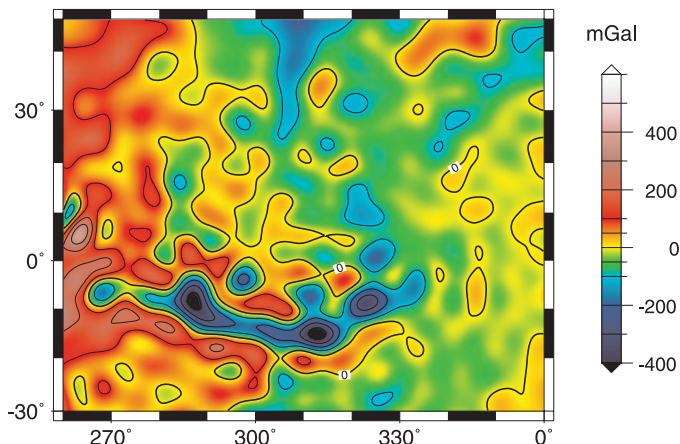


Fig. 6. Gravity of the Valles Marineris canyons system and Chryse outflow channels (7).



References and Notes

1. G. L. Tyler *et al.*, *J. Geophys. Res.* **97**, 7759 (1992); A. A. Albee, F. D. Palluconi, R. E. Arvidson, *Science* **279**, 1671 (1998).
2. Doppler radio tracking observations of MGS (primary) and selected Mariner 9 and Viking 1 and 2 data were used. MGS observations are "two-way" at 7.9 and 8.4 GHz. Mariner 9 and Viking were 2.1 and 2.3 GHz, respectively. The accuracy of MGS is better than 0.1 mm s⁻¹ for an averaging time of 10 s.
3. Independent models were developed at NASA Goddard Space Flight Center (GSFC) and the Jet Propulsion Laboratory (JPL). The fields were solved (33) to degree and order 70 (7) and 75 (6), but are shown and interpreted only to degree and order 48, corresponding to a half-wavelength resolution of 220 km. Peak values of gravitational features depend on the effective resolution of the gravity model.
4. G. Balmino, B. Moynot, N. Vales, *J. Geophys. Res.* **87**, 9735 (1982); D. E. Smith *et al.*, *ibid.* **98**, 20871 (1993); A. S. Konopliv and W. L. Sjogren, "The JPL Mars gravity field, Mars50c, based upon Viking and Mariner 9 Doppler Tracking data," *JPL Publ.* 95-5 (Jet Propulsion Laboratory, Pasadena, CA, 1995).
5. P. B. Esposito *et al.*, in *Mars*, H. H. Kieffer, B. M. Jakosky, C. W. Snyder, M. S. Matthews, Eds. (Univ. of Arizona Press, Tucson, 1992), pp. 209-248.
6. W. L. Sjogren, D. Yuan, A. S. Konopliv, *Eos* **80**, 204 (abstr.) (1999).
7. D. E. Smith, F. G. Lemoine, M. T. Zuber, *ibid.*, p. 204 (abstr.) (1999).
8. Gravity potential of the hydrostatic figure can be represented by even zonal harmonics. For Mars, about 95% of the degree 2 term is estimated to be due to the hydrostatic figure [W. A. Heiskanen and H. Moritz, *Physical Geodesy* (Freeman, New York, 1967); W. M. Folkner *et al.*, *Science* **278**, 1749 (1997); M. T. Zuber and D. E. Smith, *J. Geophys. Res.* **102**, 28673 (1997)]. The remaining 5% corresponds to nonhydrostatic contributions associated with surface processes and internal dynamics.
9. F. G. Lemoine *et al.*, "The development of the joint NASA GSFC and the National Imagery and Mapping Agency (NIMA) geopotential model EGM96," *NASA/TP-1998-206861* (1998).
10. Commission errors at the poles and the equator are ~10 mgal and ~20 mgal, respectively. The errors are larger in regions of major anomalies (Table 2), such as Olympus Mons, where the error is ~100 mgal.
11. D. L. Turcotte, R. J. Willemann, W. F. Haxby, J. Norberry, *J. Geophys. Res.* **86**, 3951 (1981).
12. D. E. Smith *et al.*, *Science* **284**, 1495 (1999).
13. The areoid is a surface of constant gravity potential on Mars. Areoid anomalies are deviations from a specified equipotential surface defined here as the potential of the mean equatorial radius of Mars of 3396.0 km.
14. M. T. Zuber, D. E. Smith, F. G. Lemoine, G. A. Neumann, *Science* **266**, 1839 (1994).
15. M. H. Acuña *et al.*, *ibid.* **284**, 790 (1999); J. E. P. Connerney *et al.*, *ibid.* **284**, 794 (1999).

16. M. T. Zuber *et al.*, *ibid.* **282**, 2053 (1998).
17. C. L. Johnson *et al.*, in preparation.
18. In early martian history (>4 billion years), volcanic material flooded the low northern hemisphere [M. H. Carr, *The Surface of Mars* (Yale Univ. Press, New Haven, CT, 1981)], and produced vast, smooth plains [D. E. Smith *et al.*, *Science* **279**, 1686 (1998)].
19. Modeling gravity and topography of lunar basins indicates that several are superisostatic, and estimated thickness of basaltic mare fill is inadequate to explain the magnitude of the central positive anomaly (14, 22) [H. J. Melosh, *Impact Cratering: A Geologic Process* (Oxford Univ. Press, New York, 1989)].
20. Where lithosphere viscosity decreases with depth, longer wavelength loads relax more rapidly than shorter wavelength loads.
21. S. R. Bratt, S. C. Solomon, J. W. Head, *J. Geophys. Res.* **90**, 12415 (1985); A. S. Konopliv *et al.*, *Science* **281**, 1476 (1998).

22. G. A. Neumann, M. T. Zuber, D. E. Smith, F. G. Lemoine, *J. Geophys. Res.* **101**, 16841 (1996).
23. G. A. Neumann and M. T. Zuber, *Lunar Planet. Sci. Conf. XXVIII*, 1713 (1997).
24. G. E. McGill, *J. Geophys. Res.* **94**, 2753 (1989).
25. M. T. Zuber *et al.*, *Geophys. Res. Lett.* **25**, 4393 (1998).
26. D. E. Wilhelms and S. W. Squyres, *Nature* **309**, 138 (1984); H. V. Frey, and R. A. Schultz, *Geophys. Res. Lett.* **15**, 229 (1988).
27. D. L. Turcotte and G. Schubert, *Geodynamics: Applications of Continuum Physics to Geological Problems* (Wiley, New York, 1982).
28. R. P. Comer, S. C. Solomon, J. W. Head, *Rev. Geophys.* **23**, 61 (1985); S. C. Solomon *et al.*, *Lunar Planet. Sci. Conf. XXIX*, 1389 (1998).
29. S. Anderson and R. E. Grimm, *J. Geophys. Res.* **103**, 11113 (1998).
30. A. M. C. Sengor and K. Burke, *Geophys. Res. Lett.* **5**, 419 (1978).
31. D. H. Scott and K. L. Tanaka, *U.S. Geol. Surv. Map I-1802-A* (1986); R. Greeley and J. E. Guest, *U.S. Geol. Surv. Map I-1802-B* (1987).
32. R. A. Schultz and H. V. Frey, *J. Geophys. Res.* **95**, 14175 (1990).
33. W. M. Kaula, *Theory of Satellite Geodesy, Applications of Satellites to Geodesy* (Blaisdell, Waltham, MA, 1966).
34. The data used in this study will be deposited with the NASA Planetary Data System (<http://pds-geophys.wustl.edu/pds/>) 1 October 1999. We gratefully acknowledge P. Priest, S. Abbate, S. Asmar, and M. Connolly for the observations; G. Neumann, S. Fricke, and D. Yuan for data analysis; and R. Simpson and J. Twicken for data assessment and archiving. We thank the MGS spacecraft and operation teams at JPL and Lockheed-Martin Astronautics in the management of the MGS mission and M. Zuber for stimulating and helpful discussions regarding the interpretation. This investigation was supported by the NASA Mars Global Surveyor Project.

29 July 1999; accepted 8 September 1999

Sulfuric Acid on Europa and the Radiolytic Sulfur Cycle

R. W. Carlson,^{1*} R. E. Johnson,² M. S. Anderson¹

A comparison of laboratory spectra with Galileo data indicates that hydrated sulfuric acid is present and is a major component of Europa's surface. In addition, this moon's visually dark surface material, which spatially correlates with the sulfuric acid concentration, is identified as radiolytically altered sulfur polymers. Radiolysis of the surface by magnetospheric plasma bombardment continuously cycles sulfur between three forms: sulfuric acid, sulfur dioxide, and sulfur polymers, with sulfuric acid being about 50 times as abundant as the other forms. Enhanced sulfuric acid concentrations are found in Europa's geologically young terrains, suggesting that low-temperature, liquid sulfuric acid may influence geological processes.

Europa is unique among Jupiter's moons. It is differentiated (1) with an icy crust that may melt from tidal heating to produce a subsurface ocean (2). The surface may be young and renewed by solid state convection (3) or ex-

trusion of solid or liquid material from below (4). Europa's surface exhibits bright, icy plains and younger, darker mottled terrain (4). Linear features with different morphologies crisscross the surface. These long (>1000 km), narrow (10 to 20 km) features often show bright central bands flanked by bands of darker material ("triple bands"). Because Europa is within Jupiter's energetic magnetosphere, the surface is subject to intense bombardment by high-energy plasma (e⁻, H⁺, Oⁿ⁺, and Sⁿ⁺) (5-7) that can alter the

¹Jet Propulsion Laboratory, California Institute of Technology, Pasadena, CA 91109, USA. ²Engineering Physics, School of Engineering and Applied Sciences, University of Virginia, Charlottesville, VA 22903-2442, USA.

*To whom correspondence should be addressed. E-mail: rcarlson@lively.jpl.nasa.gov

surface by radiolysis and ion implantation (8–10).

Europa's surface consists mainly of H₂O ice and hydrated materials (11, 12), with minor amounts of SO₂, CO₂, and H₂O₂ (9, 10, 13). Hydrated compounds on Europa were suggested by shifts and distortions of H₂O absorption bands found in spectra obtained by Galileo's near-infrared mapping spectrometer (NIMS) (11, 12). These spectra vary between two extremes (end-members), from icelike, with a symmetric absorption band at 2 μm in wavelength, to predominately hydrated, with highly distorted H₂O bands (Fig. 1A). Most NIMS spectra of Europa's surface indicate mixtures of these two end-members. Although the hydrated material is ubiquitous on Europa, there is more of it within the linear features and the dark mottled terrain (12) of Europa's trailing (in relation to orbital motion) hemisphere, which suffers the greatest plasma bombardment and implantation (5).

It was suggested (12) that Europa's spectra are similar to those of hydrated salt minerals (Fig. 1B) such as epsomite (MgSO₄·7H₂O), magnesium hexahydrate (MgSO₄·6H₂O), and natron (Na₂CO₃·10H₂O). Fits based on combining spectra of several salts were suggested to indicate a subsurface ocean (12), with salt minerals being formed on Europa's surface (14) by extrusion of subsurface brine that evaporates to form salt pans, similar to terrestrial deposits. However, identification of specific hydrates in the spectra is not unique (12). The presence of H₂O₂ and SO₂ in the icy surface of Europa suggests that sulfuric acid (H₂SO₄), a common photochemical product in the atmospheres of Earth and Venus, might be formed on Europa. Here, we present laboratory spectra showing that NIMS observations of the european surface are consistent with the presence of hydrated H₂SO₄ and show that H₂SO₄ is part of a radiolytic sulfur cycle.

Frozen H₂SO₄ hydrates occur as H₂SO₄·nH₂O, where n = 1, 2, 3, 4, 6.5, and 8 (15–17). We investigated the n = 4, 6.5, and 8 hydrates by freezing stoichiometric solutions and obtaining their infrared (IR) reflectance spectra. The solutions contained spectrally neutral diamond powder to produce diffusely reflecting media. Samples with various grain sizes (effective diameters of ~5 to ~50 μm) were prepared, and spectra were obtained for temperatures between ~80 K and their melting points (~220 to 230 K). The spectra (Fig. 1C) of H₂SO₄·6.5H₂O and H₂SO₄·8H₂O are similar and show little variation with temperature. The hydration bands of H₂SO₄·4H₂O were found to be less distinct than those for the n = 6.5 and 8 hydrates and unlike those in Europa's spectra. Laboratory spectra of H₂SO₄·8H₂O are similar to the spectrum of Europa's hydrated material (Fig. 1D) and provide the best match yet found for any single compound (18).

The small differences between the Europa and laboratory spectra (Fig. 1D) may be due to several effects. (i) The Europa spectrum also contains H₂O ice features, inclusion of which may improve the comparison, particularly in the 1.2- to 1.4-μm region. (ii) The wavelengths of reflectance minima for hydration bands are reduced by ion irradiation and partial dehydration. Shifts of ~0.02 μm were produced by proton irradiation (19), and spectra of partially dehydrated sulfates exhibit shifts of 0.04 μm (11). Such effects may be responsible for the small mismatch of band positions found in the Europa and laboratory spectra. (iii) The grain sizes of the laboratory samples may be different from those on Europa's surface. (iv) Other hydrates may also be present in Europa's spectrum.

With the above effects, the match to the NIMS spectra suggests that H₂SO₄·nH₂O (n = 6.5 and 8) is a major component of Europa's optically sensed surface. The opti-

cal sampling depth is a few grain diameters [~60 μm on Europa (9)], so we adopted 200 μm as the effective sampling depth. The number of H₂SO₄ hydrated molecules for Europa's surface area (whose spectrum is given in Fig. 1D) is ~7 × 10¹⁹ cm⁻² (200 μm)⁻¹. The average number of H₂SO₄ molecules for Europa's trailing hemisphere is ~3 × 10¹⁹ cm⁻² (200 μm)⁻¹.

NIMS spectra of hydrated regions are featureless in the 3- to 5-μm region. We measured the mid-IR diffuse reflectance of a frozen H₂SO₄·8H₂O sample and found no spectral features in this range, consistent with NIMS spectra. We also measured the ultraviolet (UV) properties of H₂SO₄·8H₂O. An absorption band was found at 190 nm, with weaker absorption extending to 240 nm. A UV spectrum of Europa's trailing side (13) shows a possible absorption onset at 225 nm, which could be due to H₂SO₄ hydrate absorption. However, SO₂ also has an absorption band beginning at these same wavelengths (20), and because a longer wavelength SO₂ band appears in Europa's UV spectrum, the 225-nm onset could be due to SO₂ alone. Therefore, Europa's UV spectrum is consistent with H₂SO₄ hydrates existing on Europa.

The H₂SO₄ concentration correlates with Europa's dark material. Sulfuric acid hydrates are visually colorless, so the dark material is a related compound acting as a source, sink, or both. Sulfur has been suggested as a constituent for Europa's dark material (4, 21). We compare the visible reflectance of Europa's trailing side (22) to the reflectance of polymerized sulfur produced by radiolysis and photolysis (23–25)

Fig. 1. IR reflectance spectra of Europa and candidate surface materials. (A) NIMS Europa end-member spectra. Ice abundance is much greater than hydrate (solid line), and hydrate abundance is much greater than ice (line with circles). (B) Evaporite salt minerals (12). (C) Spectra of H₂SO₄·nH₂O for various n, grain size (d), and temperature (T): n = 8, d = 5 μm, and T = 80 K, offset vertically by 0.10 (short-dashed line); n = 8, d = 50 μm, and T = 80 K, offset vertically by 0.05 (long-dashed line); n = 8, d = 50 μm, and T = 140 K (solid line); and n = 6.5, d = 50 μm, and T = 80 K (dotted line). (D) Comparison of Europa's hydrate spectrum [line with circles, from (A)] and H₂SO₄·8H₂O at T = 140 K and d = 50 μm, normalized at 1.1 μm [solid line, from (C)].

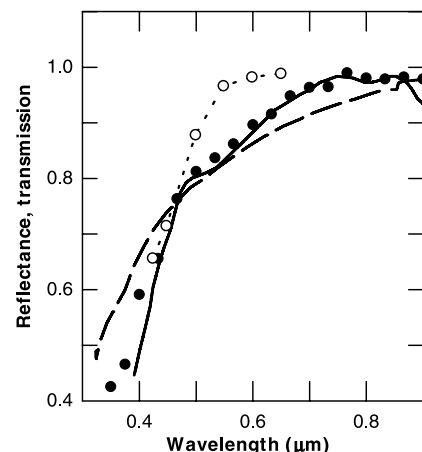
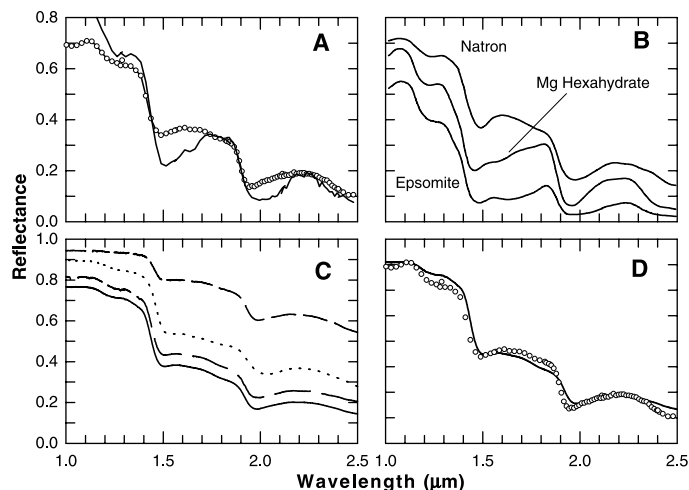


Fig. 2. Reflectance spectra of Europa's trailing side compared to photolyzed and radiolyzed sulfur compounds. We compare Europa's spectrum (22) (solid dots); photolyzed H₂S + 10H₂O (23) (solid line); the transmission of ion-irradiated SO₂ (24), assumed here to approximate the reflectance when the same number of molecules is in the optical path (dashed line); and the SO₂⁺-irradiated H₂O ice (25), assumed to represent implanted and irradiated sulfur in H₂O ice (dotted line with circles).

(Fig. 2). The shape of Europa's spectrum (approximately bilinear, with a breakpoint at 0.5 μm) is similar to the laboratory spectra and suggests that altered sulfur compounds are present on the surface. Because the visible reflectance of these materials and Europa are about the same, we estimate that the amount of polymerized sulfur in Europa's optically sampled layer is $\sim 4 \times 10^{17}$ atoms cm^{-2} ($200 \mu\text{m}$) $^{-1}$ (24, 25). Therefore, we suggest three chemical reservoirs for Europa's sulfurous compounds: (i) polymerized sulfur, (ii) SO_2 , with optically sensed surface densities of $\sim 2 \times 10^{17}$ cm^{-2} ($200 \mu\text{m}$) $^{-1}$ (13), and (iii) H_2SO_4 hydrate. Because extensive radiation dosage occurs to depths of 200 μm in geologically short times (6), these reservoirs are in radiation-induced equilibrium, with sulfur being continuously cycled among these forms.

The production of H_2SO_4 hydrate in this radiolytic cycle can be estimated with the G value, the number of molecules produced per 100 eV of energy absorbed. Laboratory radiolysis of sulfur hydrosols produces sulfate (26), and irradiation of polymerized sulfur in Europa's ice may be similar. For hydrosols, $G(\text{SO}_4) \approx 0.6$ and applies to concentrations that are $< 10^{-4}$ of Europa's polymerized sulfur concentration. However, these data apply to liquid suspensions and not to frozen mixtures. Irradiation of a 10:7 mixture of $\text{H}_2\text{O}:\text{SO}_2$ ice produced compounds whose complicated 2.5- to 25- μm spectra contain features that may be due to H_2SO_4 hydrates (27). Radiolysis of SO_2 ice produces sulfur, sulfate, and (predominately) SO_3 (28). In the presence of H_2O , SO_3 rapidly forms H_2SO_4 in an exothermic reaction (29). The G value for SO_2 in H_2O ice is not available, so we used the value for SO_3 production in pure SO_2 ice ($G \approx 5$) (28). With this G value, Europa's SO_2 concentration, and a value of $\sim 5 \times 10^{10}$ $\text{keV s}^{-1} \text{cm}^{-2}$ for Europa's irradiation flux (6), we obtained an H_2SO_4 production of $\sim 1 \times 10^9$ $\text{s}^{-1} \text{cm}^{-2}$. Irradiation of polymerized sulfur in H_2O ice and associative reactions of SO_2 with H_2O can also produce H_2SO_4 , so the above rate is a lower limit. The optically observed H_2SO_4 surface concentration [$\sim 3 \times 10^{19}$ cm^{-2} ($200 \mu\text{m}$) $^{-1}$] can be formed from SO_2 and polymerized sulfur in $< 10^4$ years.

Sulfuric acid is quite stable under irradiation. When hydrogen is removed from H_2SO_4 , it recombines quickly (30). Destruction of SO_4 is moderated by reactions between SO_2 and H_2O_2 molecules produced during radiolysis (31). The net destruction rate of H_2SO_4 can be estimated from rates for another acid sulfate, Li_2SO_4 , which exhibits $G \approx 10^{-3}$ to 10^{-4} (32). These values are consistent with upper limits for H_2SO_4 at Europa's concentration levels (31). The high radiation stability of H_2SO_4 , particularly for the $n = 6.5$ and 8 hydrates (31), implies large concentrations of H_2SO_4 in comparison to SO_2 and polymerized sulfur. The observations show that Europa's H_2SO_4 is more abundant

than either SO_2 or polymerized sulfur by a factor of ~ 100 (assuming that the photon sampling depths are about the same). The G values, obtained for x-ray and gamma-ray irradiation, give lower bounds for destruction by energetic particles of $\sim 5 \times 10^7$ to 5×10^8 $\text{s}^{-1} \text{cm}^{-2}$. Heavy ions and UV radiation can also decompose H_2SO_4 in the upper few micrometers of the surface (6), but G values and cross sections are not available.

The original source of sulfur may be S^{n+} ions implanted from the jovian plasma. The plasma influx, $\sim 6 \times 10^7$ sulfur ions $\text{cm}^{-2} \text{s}^{-1}$ (7), provides a sufficient amount of sulfur to account for the three reservoirs in 10^4 years. However, implantation would be expected to produce a more uniform surface distribution than is observed, so if the ultimate source of sulfur is plasma implantation, then some geological process has acted to produce the observed nonuniform distribution. One possibility is the burial of implanted sulfur and its radiolytic products by solid state convection, forming a crust enriched with H_2SO_4 , SO_2 , and sulfur polymers. Subsequent convection of matter back to the surface may produce a nonuniform distribution of sulfurous material. Cracks in this crust can be filled by the extrusion of ice or liquid H_2O from below. This upwelling material can scour the crack walls, forming two layers of upward moving sulfurous till. The surface expression would be two dark bands and possibly a bright median of pure ice, accounting for the appearance of Europa's triple bands (4). Alternatively, much of the sulfurous material on Europa's surface may have been endogenic. Sulfuric acid formed internally could be geologically emplaced onto the surface. The extrusion of salt-rich brine (12) may have provided sulfate salts to the surface, where proton implantation can replace salt mineral cations to form H_2SO_4 . Radiolysis of such evaporite salt minerals should also produce MgO , MgOH , $\text{Mg}(\text{OH})_2$, Na_2O , and NaOH (14, 33). However, hydroxides exhibit 1.4- μm bands (34) that are not evident in NIMS spectra (Fig. 1A) and imply hydroxide concentration limits of $< 10\%$.

The melting point of H_2SO_4 solutions can be as much as 55 K lower than that of pure H_2O ice (15), so liquid H_2SO_4 may be formed more readily by tidal heating compared to melted brine. Enhanced H_2SO_4 concentrations are associated with geological structures whose formation may have been affected by the presence of liquid H_2SO_4 . Sulfuric acid can supercool to 150 K (16), possibly facilitating cryovolcanic activity. The acid is also an electrical conductor and may contribute to Europa's magnetic signature (35).

References and Notes

1. J. D. Anderson et al., *Science* **281**, 2019 (1998).
2. M. H. Carr et al., *Nature* **391**, 363 (1998).
3. R. T. Pappalardo et al., *ibid.*, p. 365.
4. R. Greeley et al., *Icarus* **135**, 4 (1998).

5. M. K. Pospieszalska and R. E. Johnson, *ibid.* **78**, 1 (1989).
6. J. F. Cooper et al., in preparation.
7. W. H. Ip, *Icarus* **120**, 317 (1996).
8. R. E. Johnson and T. I. Quickenden, *J. Geophys. Res.* **102**, 10985 (1997).
9. R. W. Carlson et al., *Science* **283**, 2062 (1999).
10. A. L. Lane, R. M. Nelson, D. L. Matson, *Nature* **292**, 38 (1981).
11. R. W. Carlson et al., in *Highlights of Astronomy*, vol. 11B, J. Anderson, Ed. (Kluwer Academic, Norwell, MA, 1998), pp. 1078–1081. Band positions are given for Europa and hydrated minerals, including $\text{MgSO}_4 \cdot n\text{H}_2\text{O}$, $n < 1$ to $n \approx 7$.
12. T. B. McCord et al., *Science* **280**, 1242 (1998); T. B. McCord et al., *J. Geophys. Res.* **104**, 11827 (1999).
13. K. S. Noll, H. A. Weaver, A. M. Gonnella, *J. Geophys. Res.* **100**, 19057 (1995).
14. D. L. Hogenboom et al., *Icarus* **115**, 258 (1995).
15. F. J. Zeleznik, *J. Phys. Chem. Ref. Data* **20**, 1157 (1991). The octahydrate is metastable above 200 K. The octahydrate and hemihydrate structures are $(\text{H}_5\text{O}_2)_2\text{SO}_4 \cdot 4\text{H}_2\text{O}$ and $(\text{H}_5\text{O}_3)(\text{H}_5\text{O}_2)\text{SO}_4 \cdot 1.5\text{H}_2\text{O}$, respectively [D. Mootz and A. Merschenz-Quack, *Z. Naturforsch. B* **42**, 1231 (1987)].
16. S. T. Martin et al., *J. Phys. Chem. B* **101**, 5307 (1997).
17. Samples prepared by rapid freezing are amorphous. Preparation of crystalline samples requires repeated thermal cycling [A. B. Yaroslavtsev et al., *Russ. J. Inorg. Chem.* **28**, 1558 (1983)].
18. For example, with the normalization of Fig. 1D, the root mean square deviation for $\text{H}_2\text{SO}_4 \cdot 8\text{H}_2\text{O}$ is 2%, compared to 15, 7, and 3% for $\text{MgSO}_4 \cdot 7\text{H}_2\text{O}$, $\text{MgSO}_4 \cdot 6\text{H}_2\text{O}$, and $\text{Na}_2\text{CO}_3 \cdot 10\text{H}_2\text{O}$, respectively.
19. D. B. Nash and F. P. Fanale, *Icarus* **31**, 40 (1977).
20. B. A. Thompson, P. Harteck, R. R. Reeves Jr., *J. Geophys. Res.* **68**, 6431 (1963).
21. T. V. Johnson et al., *ibid.* **88**, 5789 (1983); M. L. Nelson et al., *Icarus* **65**, 129 (1986); R. E. Johnson et al., *ibid.* **75**, 423 (1988); J. R. Spencer, W. M. Calvin, M. J. Person, *J. Geophys. Res.* **100**, 19049 (1995).
22. W. M. Calvin et al., *J. Geophys. Res.* **100**, 19041 (1995). The geometric albedo was multiplied by 1.5 to approximate the reflectance of a uniformly diffuse plane reflector [D. L. Harris, in *Planets and Satellites*, G. P. Kuiper and M. M. Middlehurst, Eds. (Univ. of Chicago Press, Chicago, 1961), chap. 8].
23. L. A. Lebofsky and N. B. Fegley Jr., *Icarus* **28**, 379 (1976).
24. G. Strazzulla, G. Leto, M. E. Palumbo, *Adv. Space Res.* **13**, 189 (1993). Measurements were for a D^+ irradiated film of SO_2 containing 5×10^{17} atoms cm^{-2} .
25. D. J. O'Shaughnessy, J. W. Boring, R. E. Johnson, *Nature* **333**, 240 (1988). The number of sulfur atoms implanted and irradiated (as SO_2^+ molecules, which break up on impact) was $3 \times 10^{17} \text{cm}^{-2}$ [see correction by N. J. Sack et al., *Icarus* **100**, 534 (1992)].
26. G. W. Donaldson and F. J. Johnston, *J. Phys. Chem.* **72**, 3552 (1968); see also E. M. Nanobashvili and L. P. Beruchashvili, in *Proceedings of the First All-Union Conference on Radiation Chemistry, Primary Acts in Radiation Chemical Processes* (Consultants Bureau, New York, 1957), pp. 69–72; E. M. Nanobashvili et al., in *Proceedings of the Second All-Union Conference on Radiation Chemistry*, M. R. Quastel, Ed. (Israel Program for Scientific Translations, Jerusalem, 1964), pp. 159–162.
27. M. H. Moore, private communication.
28. ———, *Icarus* **59**, 114 (1984).
29. J. T. Jayne et al., *J. Phys. Chem. A* **101**, 10000 (1997).
30. E. R. Johnson and A. O. Allen, *J. Am. Chem. Soc.* **74**, 4147 (1952).
31. C. J. Hochanadel, J. A. Ghormley, T. J. Sworski, *ibid.* **77**, 3215 (1955).
32. T. Sasaki et al., *J. Chem. Phys.* **68**, 2718 (1978).
33. R. E. Johnson, R. M. Killen, J. H. Waite Jr., W. S. Lewis, *Geophys. Res. Lett.* **25**, 3257 (1998).
34. R. N. Clark et al., *J. Geophys. Res.* **95**, 12653 (1990).
35. K. K. Khurana et al., *Nature* **395**, 777 (1998).
36. Portions of this work were performed at the Jet Propulsion Laboratory, California Institute of Technology, under contract with NASA, through the NASA Jupiter System Data Analysis Program and the Galileo Project.

23 June 1999; accepted 1 September 1999